



ELSEVIER

Journal of Luminescence 94–95 (2001) 113–117

JOURNAL OF  
LUMINESCENCE

www.elsevier.com/locate/jlumin

# Crystal growth, EPR and site-selective laser spectroscopy of $Gd^{3+}$ -activated $LiCaAlF_6$ single crystals

R.Yu. Abdulsabirov<sup>a</sup>, M.A. Dubinskii<sup>b</sup>, S.L. Korableva<sup>a</sup>, A.K. Naumov<sup>a</sup>,  
V.V. Semashko<sup>a,\*</sup>, V.G. Stepanov<sup>a</sup>, M.S. Zhuchkov<sup>a</sup>

<sup>a</sup>Kazan State University, 18 Kremlyovskaja street, 420008 Kazan, Russia

<sup>b</sup>Magnon, Inc., 11710 Reisterstown Road S204A, Reisterstown, MD 21136, USA

## Abstract

$Ce^{3+}$ -activated  $LiCaAlF_6$  (LiCAF) and  $LiSrAlF_6$  (LiSAF) single crystals are the most prospective active media for directly pumped UV solid-state tunable lasers. Due to the heterovalent activation nature of these crystals, crystal spectroscopic properties as well as their laser efficiency strongly depend on the actual crystal growth conditions. In order to establish the growth-related peculiarities of activator center formation in LiCAF, concerted crystal growth, EPR and site-selective laser spectroscopic studies were performed. For EPR and optical spectroscopic studies, the  $Gd^{3+}$ -“probe” activation of LiCAF crystal was used here instead of much harder to interpret  $Ce^{3+}$  activation. The obtained results indicate that up to three types of structurally distinct  $Gd^{3+}$  centers are formed in the LiCAF crystals with their relative concentrations changing depending on the crystal growth conditions. The results are being applied for growing  $Ce^{3+}$ -activated LiCAF crystals with the desired luminescence and laser performance. © 2001 Elsevier Science B.V. All rights reserved.

**Keywords:** Rare-earth ions; Laser materials; Ultraviolet tunable lasers

## 1. Introduction

The  $LiCaAlF_6$  (LiCAF) and  $LiSrAlF_6$  (LiSAF) single crystals activated by  $Ce^{3+}$  ions are the most prospective active media for directly pumped UV solid-state tunable lasers based on interconfigurational  $5d4f^{n-1} \leftrightarrow 4f^n$  transitions of rare-earth ions [1–3]. Although due to the heterovalent activation nature of these crystals by the  $Ce^{3+}$  ion, crystal spectroscopic properties, their laser efficiency and tunability immensely depend on the actual crystal

growth conditions [4]. In-depth investigation of multi-site  $Ce^{3+}$  activation nature in these crystals would lead to improving laser materials and, thus, advanced tunable UV laser performance.

In order to establish all growth-related peculiarities of spectroscopically distinct activator center formation in LiCAF and properly interpret each optical center model, concerted crystal growth, EPR and site-selective laser spectroscopic studies were performed in this work. For EPR/optical spectroscopic studies aimed at revealing the structure of doping centers and interpreting the observed multi-site optical spectral features, the  $Gd^{3+}$  “probe” activation of LiCAF single crystals was used in lieu of a much more complex

\*Corresponding author. Tel.: +7-8432-31-5555; fax: +7-8432-41-0480.

E-mail address: semashko@bancorp.ru (V.V. Semashko).

spectroscopic interpretation of  $\text{Ce}^{3+}$  activation. To study the impact of crystal growth conditions on the paramagnetic and optical properties of  $\text{Gd}^{3+}$  in LiCAF several series of crystals largely differing by chemical constituents and other pertinent conditions were grown.

The obtained results indicate that, similar to  $\text{Ce}^{3+}$  [4], up to three types of structurally distinct types of  $\text{Gd}^{3+}$  centers are formed in LiCAF crystals with their relative concentrations changing depending on the crystal growth conditions. The models for each center were evaluated. A good correlation between the crystal growth conditions, EPR and site-selective time-resolved laser spectroscopy data was established. The results of these studies are being applied for growing the  $\text{Ce}^{3+}$ -activated LiCAF crystals with desired luminescence and laser performance.

## 2. Sample preparation and measurement techniques

Multiple  $\text{Ce}^{3+}$  impurity centers in crystals are hard to investigate, and especially make an appropriate center assignment optically, due to the short (typically 20–50 ns) upper fluorescence level lifetime, wide bandwidth and profound overlapping of the  $4f \leftrightarrow 5d$  fluorescence and absorption bands from individual structurally distinct centers, leading, in turn, to the fast inter-center excitation energy exchange [4]. As far as the EPR is concerned,  $\text{Ce}^{3+}$  ion spectrum is also not informative, because the  $\text{Ce}^{3+}$  ground state has  $S = 1/2$ , and so EPR spectrum consists of one band only—not sufficient for suggesting the appropriate impurity center model [5]. Thus, to more comprehensively understand the  $\text{Ce}^{3+}$  impurity center multi-site activation nature in LiCAF, in this work, the  $\text{Gd}^{3+}$  ion was used as a spectroscopic marker instead of  $\text{Ce}^{3+}$ . Indeed, not only  $\text{Ce}^{3+}$  and  $\text{Gd}^{3+}$  ions are in close chemical affinity, they also have close ionic radii, so it is most likely that the  $\text{Gd}^{3+}$  ions in LiCAF would occupy the positions with the same crystal environment as the  $\text{Ce}^{3+}$  dopant. Meanwhile, the  $\text{Gd}^{3+}$  ion possesses the well defined, multiple narrow-line, long-upper-level-lifetime ( $\sim 6.5$  ms in LiCAF) optical spectra as well as rich (ground

state  $^8\text{S}_{7/2}$ ,  $S = 7/2$ ), environment-sensitive EPR spectra, easily and certainly measurable at room temperature.

$\text{Gd}^{3+}$ -activated  $\text{LiCaAlF}_6$  single crystals were grown from carbon crucibles in a fluorinated atmosphere, using a modified Bridgman–Stockbarger technique (described elsewhere). Ce:LiCAF laser, similar (but much less sophisticated) to the one described in Ref. [6], with typical output pulse energy of  $\sim 1$  mJ and output spectral bandwidth of  $\sim 0.05$  nm was used for  $\text{Gd}^{3+}$  ion excitation in the 290–315 nm spectral region in our site-selective laser spectroscopy experiments. Such a source was quite appropriate for selective resonance excitation of  $\text{Gd}^{3+}$   $^6\text{P}_{7/2}$  Stark sub-levels. Due to the resonance excitation mode, fluorescence emission spectral filtering is not efficient; thus, in order to avoid PMT saturation by strong scattered excitation light, PMT was synchronously trigger-locked, so that the fluorescence intensity measurement started only  $\sim 100$   $\mu\text{s}$  after the 15 ns excitation pulse.

## 3. Experimental

$^6\text{P}_{7/2} \rightarrow ^8\text{S}_{7/2}$  transition luminescence spectrum of  $\text{Gd}^{3+}$  ions in LiCAF crystals obtained using the excitation wavelength of 311.34 nm consists of four narrow bands peaked at 310.11, 310.67, 311.04 and 311.35 nm (Fig. 1), and the spectrum

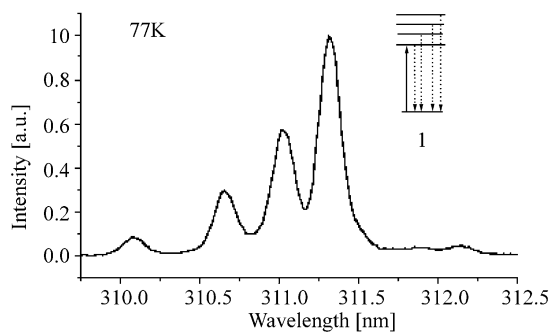


Fig. 1. Luminescence spectrum of  $\text{Gd}^{3+}$  ion in  $\text{LiCaAlF}_6$  at 77 K. Excitation wavelength is 311.34 nm. Shown on the inset is the excitation scheme of luminescence of the  $\text{Gd}^{3+}$  “type I center”.

appearance is typical for the  $Gd^{3+}$  occupying the crystal lattice the site with the point symmetry lower than cubo-octahedral. Suggested excitation—luminescence scheme for this case is indicated in Fig. 1 in the inset—luminescence takes place from all levels due to the excitation thermalization (Boltzmann). Crystal field splitting for the  $^8S_{7/2}$  ground state is very low, such that this splitting does not disturb the actual optical spectrum. Thus, in a situation when impurity center of only one type is formed in the crystal,  $Gd^{3+} \ ^6P_{7/2}$  Stark level diagram can be easily obtained, and the luminescence spectrum appearance would not depend on the excitation wavelength. In case when several types of  $Gd^{3+}$  impurity centers are formed, a finite amount of different luminescence spectra or, if overlapping takes place, then their superpositions will be observed. In order to reduce possible inter-center excitation energy exchange, low  $Gd^{3+}$  concentration ( $<0.1\%$ ) and reduced sample temperature (LNT) were used in our experiments.

Using the preliminary data on the  $Gd^{3+} \ ^6P_{7/2}$  excited Stark sub-level positions from the spectrum shown in Fig. 1,  $Gd^{3+} : LiCaAlF_6$  luminescence spectra were taken also with the excitation wavelengths set to each of the luminescence maxima separately to cause resonance excitation. No noticeable change in luminescence spectrum appearance was observed in either case. Observed temperature variation of the luminescence spectrum appearance in the 70–300°K temperature range followed the Boltzmann's population distribution over the  $^6P_{7/2}$  multiplet Stark sub-levels. Based on the above observations, the luminescence spectrum shown in Fig. 1 was interpreted as an individual spectrum of one of the structurally distinct  $Gd^{3+}$  centers in LiCAF (called here “type I spectrum” and “type I center”, correspondingly).

When excitation wavelengths were set to some positions off the luminescence peak maxima shown in Fig. 1 several additional luminescence bands were observed, which indirectly proved the multiple  $Gd^{3+}$  center formation in LiCAF. The LNT  $Gd^{3+} : LiCaAlF_6$  luminescence spectrum obtained with the excitation wavelength of 310.9 nm is shown in Fig. 2 (trace 2). In order to find an alternate center peak position the differential

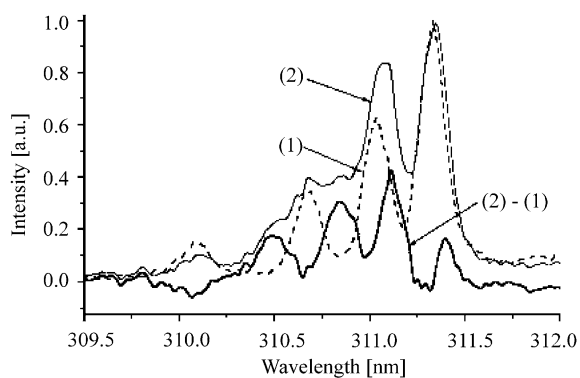


Fig. 2. Luminescence spectra of  $Gd:LiCAF$  single crystals: (1) excitation wavelength, 311.34 nm; (2) excitation wavelength 310.9 nm; (2)–(1) differential luminescence spectrum (point-by-point difference between the fluorescence intensities shown in spectra 2 and 1).

spectrum between the luminescence spectrum excited at 310.9 nm (Fig. 2, trace 2) and the “type I spectrum” excited at 311.34 nm (Fig. 2, trace 1), both normalized to a 1.0, was calculated. It is shown in Fig. 2 as trace [(2)–(1)]. As can be seen from figure, there should be at least one more four-band luminescence series with wavelengths of 310.21, 310.8, 311.13 and 311.42 nm. Using the excitation wavelength of 311.45 nm—closer to the longest wavelength maximum of the differential luminescence spectrum mentioned above—we have obtained a distinctively different luminescence spectrum which was assigned to the so-called  $Gd^{3+}$  “type II center”—a direct optical evidence of  $Gd^{3+} : LiCaAlF_6$  multi-site activation (Fig. 3). Temperature variation of the “type II center” relative luminescence band intensities in the 70–300°K temperature range was also in a good agreement with Boltzmann's population distribution over the  $^6P_{7/2}$  multiplet Stark sub-levels.

Besides the “type I” and “type II” luminescence, nearly each luminescence spectrum contained a trace amount of two additional lines peaked at 311.8 and 312.2 nm. All efforts to selectively excite solely the “type III” center, supposedly associated with these lines, have failed—it only appeared as a trace admixture to the “main” spectra described above. It is suggested that the actual concentration of the “type III” center is very low, so that its resonance excitation is inefficient, and its observed

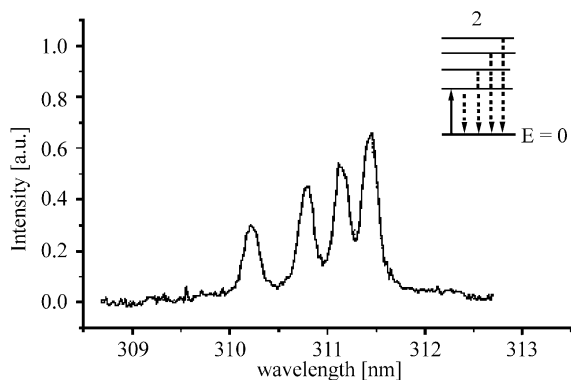


Fig. 3. Luminescence spectrum of  $Gd^{3+}$  ion in  $LiCaAlF_6$  at 77 K. Excitation wavelength 311.45 nm—"type II center".

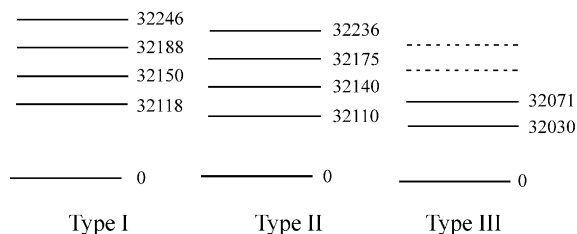


Fig. 4.  ${}^6P_{7/2}$  multiplet Stark energy sub-level diagram for the three spectroscopically distinct  $Gd^{3+}$  optical centers in  $LiCaAlF_6$  single crystal.

luminescence is mainly due to the energy transfer from the properly excited "type I" and "type II"  $Gd^{3+}$  centers.

Information on all the identified  $Gd^{3+}$   ${}^6P_{7/2}$  multiplet Stark sub-level positions in  $LiCaAlF_6$  for the three centers described above is summarized in Fig. 4.

Detailed experimental EPR studies aimed at an identification of multiple center local lattice environments, have shown that three paramagnetic center types are formed in  $Gd^{3+}$ -activated  $LiCaAlF_6$  crystals [5]. In this work, based on the tight correlation between the EPR and optical spectral features in the same  $Gd^{3+}:LiCaAlF_6$  experimental sample series, a structural center assignment was provided for all three observed center types. It was shown that "type I" centers, which have the highest concentration regardless of the growth conditions and actual growth melt

composition, can be presented as  $Gd^{3+}$  impurity center, where substitution  $Gd^{3+} \rightarrow Ca^{2+}$  is accompanied by non-local positive charge compensation. Next, lower concentration center (0.2–0.7 relative to "type I", depending on the growth conditions) is "type II" center, wherein  $Gd^{3+}$  substitutes for  $Ca^{2+}$  with local charge compensation. The least concentrated (0–0.1 relative to "type I", depending on the growth conditions and composition) is the "type III" center, which is formed wherein  $Gd^{3+}$  substitutes for  $Al^{3+}$  ions in the  $LiCaAlF_6$  host lattice. It was also found that while changing the sample growth conditions and following synchronously the EPR and luminescence intensity changes, it is possible to unambiguously assign observed fluorescence features to various center models, obtained from EPR experiments.

#### 4. Conclusions

The obtained experimental results allowed us to identify the  ${}^6P_{7/2}$  multiplet Stark energy sub-level diagrams for the three spectroscopically distinct  $Gd^{3+}$  optical centers in  $LiCaAlF_6$  single crystal. Correlation between the EPR and site-selective optical spectroscopy data also allowed to identify the lattice environment situation for each observed optical center. It was also shown that all peculiarities of multiple center formation strongly depend on crystal growth conditions as well as melt ingredients, and can be selectively controlled for obtaining some targeted spectroscopic and laser crystal properties.

#### Acknowledgements

This work was partially supported by NATO Grant HTECH. LG 970582 and by INTAS Grant 97-0787.

#### References

- [1] M.A. Dubinskii, V.V. Semashko, A.K. Naumov, R.Yu. Abdulsabirov, S.L. Korableva, J. Mod. Opt. 40 (1993) 1.

- [2] C.D. Marshall, J.A. Speth, S.A. Payne, W.F. Krupke, G.J. Quarles, V. Castillo, B.H.T. Chai, *J. Opt. Soc. Am. B* 11 (1994) 2054.
- [3] N. Sarukura, M.A. Dubinskii, Zh. Liu, V.V. Semashko, A.K. Naumov, S.L. Korableva, R.Yu. Abdulsabirov, K. Edamaksu, Y. Suzuki, T. Itoh, Y. Segawa, *IEEE J. Sel. Top. Quantum Electron.* 1 (1995) 792.
- [4] V.V. Semashko, M.A. Dubinskii, R.Yu. Abdulsabirov, A.K. Naumov, S.L. Korableva, N.K. Sherbakova, A.E. Klimovitskii, *Laser Phys.* 5 (1995) 69.
- [5] I.I. Antonova, I.N. Nizamutdinov, R.Yu. Abdulsabirov, S.L. Korableva, V.G. Stepanov, *Appl. Magn. Resonance* 13 (1997) 579.
- [6] M.A. Dubinskii, K.L. Schepler, V.V. Semashko, R.Yu. Abdulsabirov, S.L. Korableva, A.K. Naumov, *J. Mod. Opt.* 45 (1998) 1993.